

# Visualizing Electrical Breakdown and ON/OFF States in Electrically Switchable Suspended Graphene Break Junctions

Hang Zhang,<sup>†,§</sup> Wenzhong Bao,<sup>†,§</sup> Zeng Zhao,<sup>†</sup> Jhao-Wun Huang,<sup>†</sup> Brian Standley,<sup>‡</sup> Gang Liu,<sup>†</sup> Fenglin Wang,<sup>†</sup> Philip Kratz,<sup>†</sup> Lei Jing,<sup>†</sup> Marc Bockrath,<sup>\*,†,‡</sup> and Chun Ning Lau<sup>\*,†</sup>

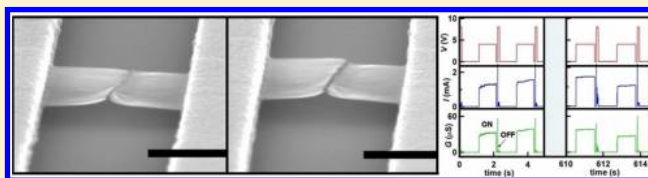
<sup>†</sup>Department of Physics and Astronomy, University of California, Riverside, California 92521, United States

<sup>‡</sup>Department of Applied Physics, California Institute of Technology, Pasadena, California 91125, United States

## Supporting Information

**ABSTRACT:** Narrow gaps are formed in suspended single- to few-layer graphene devices using a pulsed electrical breakdown technique. The conductance of the resulting devices can be programmed by the application of voltage pulses, with voltages of 2.5 to  $\sim 4.5$  V, corresponding to an ON pulse, and  $\sim 8$  V, corresponding to an OFF pulse. Electron microscope imaging of the devices shows that the graphene sheets typically remain suspended and that the device conductance tends to zero when the observed gap is large. The switching rate is strongly temperature dependent, which rules out a purely electromechanical switching mechanism. This observed switching in suspended graphene devices strongly suggests a switching mechanism via atomic movement and/or chemical rearrangement and underscores the potential of all-carbon devices for integration with graphene electronics.

**KEYWORDS:** Suspended graphene, switches, electromigration, nonvolatile memory, break junction



Long-term archival information storage is an open challenge with a variety of approaches proposed,<sup>1</sup> including periodic migration to new media. However, such approaches require constant effort to avoid loss due to data errors caused by finite storage medium lifetime. A nonvolatile means of storing information densely which is stable for extended time periods is therefore highly desirable. One approach to address this issue is to store information in the arrangement of atoms rather than electrical charges. Previous work has shown the electromigration of metallic particles in multiwalled carbon nanotubes (MWNTs).<sup>2,3</sup> More recently, conductance switching was observed in graphene and graphitic break junctions, and the proposed switching mechanism was the formation and breakdown of carbon chains or filaments.<sup>4,5</sup> However, later works reported cyclable conductance switching in devices solely consists of electrodes on SiO<sub>2</sub> interrupted by nanogaps,<sup>6,7</sup> thus it remains controversial whether the switching behavior in substrate-supported devices is intrinsic or merely arising from the underlying substrate.

To determine the role of the substrate in producing the switching behavior and to gain more insight into electromigration and switching in graphene, we study switching in suspended graphene layers that are isolated from the substrate.<sup>8–10</sup> We demonstrate that switching in such suspended graphene break junctions has similar behavior to that of substrate-supported devices. The switches are formed by a breakdown of graphene which leaves a small gap, using a sequential breakdown technique. The junction resistance can be controlled by the application of voltage pulses, with 4 V corresponding to an ON pulse that decreases the device resistance and 8 V corresponding to an OFF pulse that

increases the device resistance. The devices can be cycled up to hundreds of times before becoming inoperative. Scanning electron microscopy (SEM) imaging of the gap in the ON and OFF states shows a larger gap in the OFF state than the ON state. The similarity of the switching characteristics in suspended devices strongly suggests that the switching mechanism is the same as on substrate supported samples (though oxide breakdown cannot be unequivocally excluded). The switching rate depends strongly on temperature, which indicates that atomic motion, chemical rearrangement, or both are essential to the switching mechanism.

Few-layer graphene sheets (typically 1–5 layers thick) are mechanically exfoliated over Si substrates covered by a layer of 300 nm thick SiO<sub>2</sub> and identified by optical microscopy.<sup>11</sup> The switch devices are fabricated with two different methods: (i) Using electron beam lithography (EBL) to fabricate the device on a graphene sample on the SiO<sub>2</sub>/Si substrate and then etching  $\sim 120$  nm SiO<sub>2</sub> under the graphene flakes by dipping the device into a buffered oxide etch solution;<sup>9,10</sup> and (ii) graphene is exfoliated onto substrates that are prepatterned with trenches, which are 250 nm deep and 2.5–5  $\mu\text{m}$  wide. Source and drain electrodes that consist of 10 nm of Ti and 70 nm of Au are deposited by evaporation through a shadow mask,<sup>12</sup> which is aligned carefully with the edge of the trenches. This approach minimizes the risk of sample collapse during the conventional EBL procedure. A completed device is shown in

**Received:** September 10, 2011

**Revised:** March 15, 2012

the inset to Figure 1a, while the main panel plots the current  $I$  and the voltage  $V$  applied to the device versus time.  $I$  is

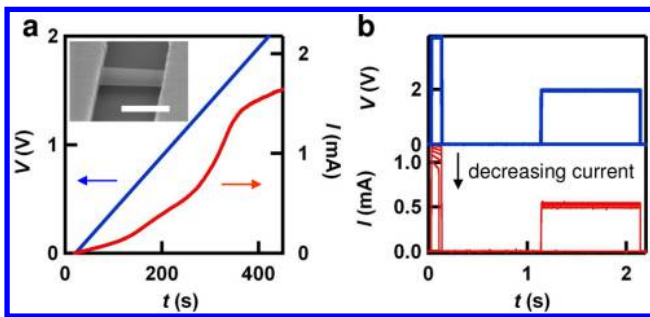


**Figure 1.** (a) The  $IV$ -time curve of a suspended graphene device. The blue curve indicates the bias voltage, and the red curve indicates the corresponding current. The inset shows the SEM image of the device. The scale bar is 1  $\mu\text{m}$ . (b, upper panel) The voltage sequence which is used to break down suspended sample. The pulse voltage is 3.9 V, the test voltage after the pulse is 1.95 V. (b, lower panel) The current response of the device during breakdown. After the last pulse, the sample is completely broken, and under the test voltage (1.95 V), the corresponding current is zero.

approximately linear in  $V$  up to  $\sim 0.5$  V, with a two-terminal conductance  $G \sim 0.5$  mS.

To create the switch, we perform the breakdown step using a modification of the electromigration technique that was reported previously.<sup>4</sup> The completed device is placed in a high vacuum, typically  $\sim 10^{-6}$  Torr, and voltage pulses ( $\sim 4$  V, typical duration 0.1 s) are applied. These pulses sequentially reduce the device conductance until it becomes zero (Figure 1b). The typical breaking current density is  $\sim 2$  mA/ $\mu\text{m}$ . Figure 2a–c shows the breakdown of another device. The device

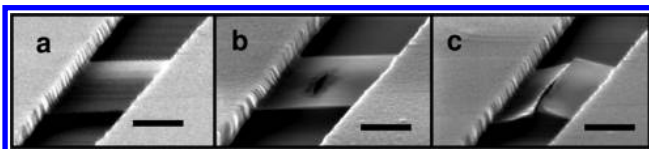


**Figure 2.** (a) A suspended sample before breakdown and (b) the broken region started from the center and expanded. The image was taken after a 3 V pulse was applied. (c) After increasing the amplitude of the pulse voltage, the sample was completely broken but still free-standing. The image was taken after an 8 V pulse was applied. The scale bar indicates 500 nm.

began its breakdown near the geometric center, and the broken region expanded upon further application of voltage until the breakdown was complete (Figure 2c). An in situ SEM video of the breakdown process is available as Supporting Information. While breakdown often began at the center, for some samples, the breakdown began at the edge but was still centrally located relative to the electrodes. This suggests that the device temperature plays a critical role in the breakdown,<sup>13,14</sup> though it is not the only factor. Other factors, such as fluctuations and defects, are also likely to be important parameters during electromigration.

Figure 3a shows the  $IV$  characteristic of a device following a successful breakdown. When the voltage is swept from  $-8$  to  $+8$  V, at first the current is zero. When the voltage is  $\sim 4$  V, the current rises, often by a series of step-like current jumps, indicating that the device is entering the “ON” state. As the

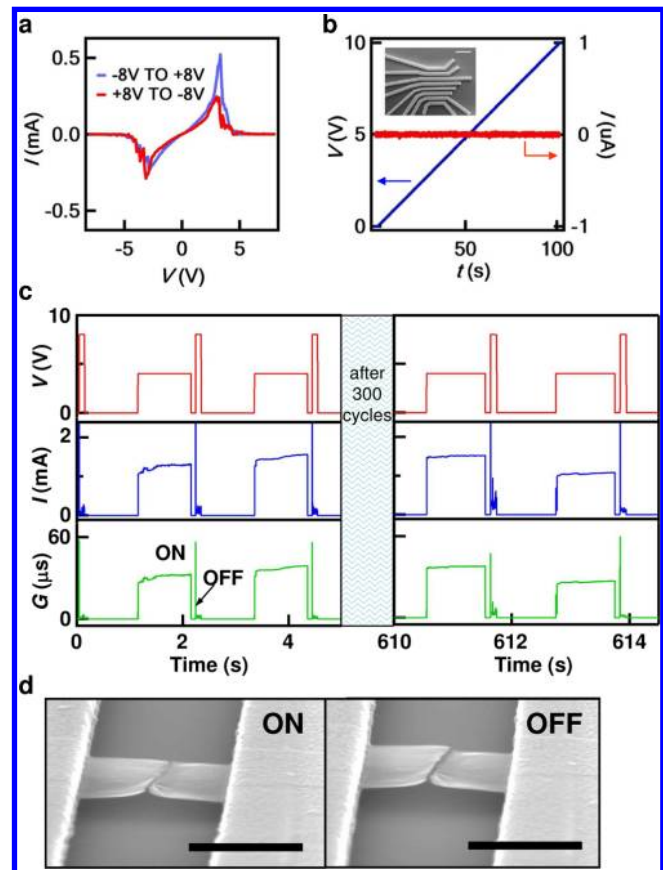


**Figure 3.** (a) The  $IV$  curve after breakdown. The voltage ramp from  $-8$  to  $+8$  V is shown as the blue curve, and the voltage ramp back from  $+8$  V to  $-8$  V is shown as the red curve. (b) The  $IV$ -time curve of a pure  $\text{SiO}_2$  device, which has the same geometry and etching procedure as the device shown in Figure 1a, without the presence of graphene. The blue curve indicates the voltage, and the red curve indicates the current. The current is approximately zero for voltage up to 10 V. The inset shows the SEM image of the control device. The scale bar is 10  $\mu\text{m}$ . (c) The repeatability of the switching behavior. From top to bottom, the panels display the applied voltage  $V$ , the current response  $I$ , and the device conductance  $G = I/V$  as a function of time  $t$ , respectively. Left panel: initial behavior. Right panel: after 300 switching cycles. (d) The SEM images of ON and OFF state for a different device. The scale bar is 1  $\mu\text{m}$ .

voltage is raised further, the device conductance decreases to zero, turning the device “OFF.” The sweep in the reverse direction from  $+8$  to  $-8$  V shows similar behavior. We note that the high vacuum is crucial for producing an operable switch device, presumably because of the removal of molecules that may contaminate or react with graphene devices, such as oxygen or water vapor. To exclude the possibility that the substrate contributes to the measured current by a parallel conduction path, we made a control device with the same exact fabrication procedure, including electrodes that are partially released from the substrates via etching, but without the graphene. These devices showed little or no measurable current up to the maximum voltage (10 V) used in our experiments (Figure 3b). Breakdown did occur, however, at significantly higher voltages  $\sim 210$  V. This demonstrates the presence of the graphene layer is essential for obtaining a measurable current within the 10 V voltage range employed in the experiment.

The switching behavior in the suspended devices was reproducible, and the most stable devices could be switched

many times. The switching behavior is shown in Figure 3c. Applying an ON pulse of 4 V switches the device “ON”, with typical conductance  $G \sim 25\text{--}40 \mu\text{S}$ ; an OFF pulse of 8 V, on the other hand, reduces the conductance to  $\sim 1 \mu\text{S}$ . This behavior in suspended devices is very similar to that from single-layer graphene devices that are supported on the  $\text{SiO}_2$  substrates.<sup>4</sup> This strongly suggests that the switching mechanisms are the same in both cases and that switching occurs in an all-carbon device. Notably, these switches are nonvolatile and robust. For suspended devices, they can be switched up to hundreds of cycles. As a demonstration, the device behavior after 300 cycles is shown in the right panels of Figure 3c, which is very similar to that of the first two cycles. However it was found that the number of switching cycles before the device failure was less than that of those on substrates, as one may expect for the greater degree of fragility of suspended devices.

To understand better how the switching behavior occurred, we also imaged a different device by SEM in both the ON and OFF states (Figure 3d). We note that imaging the device during the switching cycles results in device degradation and failure, which is likely due to accumulation of amorphous carbon and destabilization by the electron beam.<sup>15–17</sup> In the OFF state, a gap is clearly visible in the image, while in the ON state, the gap appears considerably smaller. This provides another indication that the current flow in the device is strictly through the graphene sheet. Since the devices are suspended and can move freely, also suggesting the possibility that there is a nanomechanical component to the switching behavior.<sup>18–21</sup> For example, due to slack in the graphene sheet, the two halves of the original sheet that are present after the breaking procedure may be electrostatically attracted to each other when the source drain voltage is applied, completing the circuit when they come into contact. This step is expected to be relatively fast. We estimate the characteristic frequency of a graphene cantilever with the typical geometry of our devices to be  $\sim 1$  MHz. This sets an upper bound for initial switch closure of  $\sim 1 \mu\text{s}$ . In this situation it is possible that there is some “switch bounce”, where the layers rebound from each other after their initial contact. This motion would be damped by the intrinsic quality factor of the graphene layers, and with a typical quality factor  $\sim 300$  at room temperature,<sup>22</sup> the motion would be reduced to the atomic scale in  $t \sim 1$  ms. Note that this estimate neglects dissipation by the collisions themselves<sup>23</sup> and is therefore an upper bound, likely an extreme one.

To further investigate the switching mechanism, we studied the temperature dependence of the switching rate. Figure 4 shows the time lapse to switch into the ON state when a square pulse of height 3.0 V is applied, using curves with a switching time approximately equal to the average time measured for events within 1 s at each temperature, plotted versus temperature in Figure 5a. The switching rates are highly temperature sensitive and show a rapid increase as the temperature is raised. A histogram of the measured switching time for a range of temperatures is plotted in Figure 5b. As the temperature is lowered, longer intervals to switch become more common and very short intervals less common. The switching rates were also measured at lower temperatures; no switching was observed at 4.5 K and indeed becomes very rare even below temperatures as large as 280 K. The long time scale for switching under appropriate conditions of  $>1$  s greatly exceeds the upper bound estimate above  $t = 1$  ms. In addition, the rate of nanomechanical switching would be expected to have little

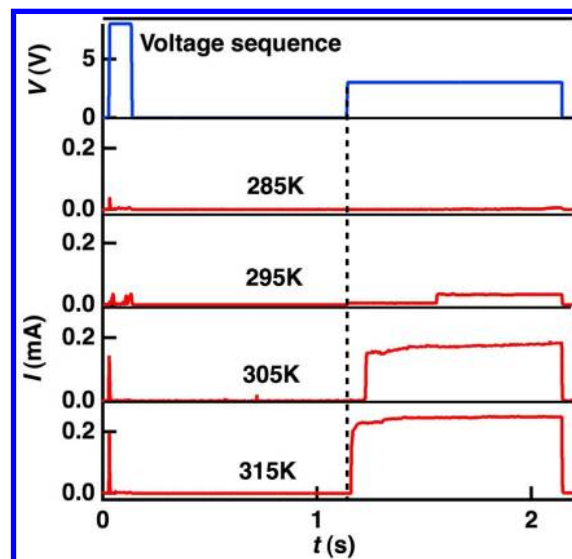


Figure 4. Typical current response versus time in a single switching cycle at different temperatures.

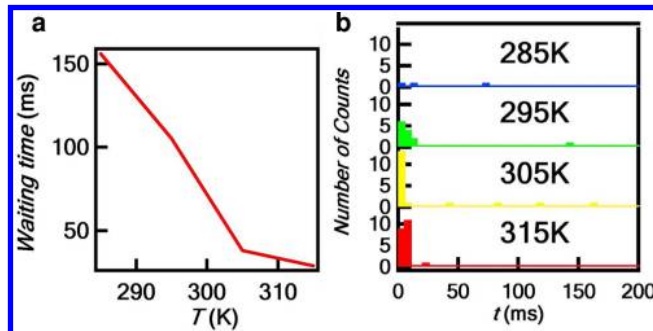


Figure 5. (a) Average waiting time vs temperature. (b) Statistical analysis of the waiting time.

temperature dependence over the the temperature range studied based on the relatively constant elastic properties of the graphene sheets. This strongly indicates that the switching rate is not limited by nanomechanical motion but rather by a step that involves the motion of atoms and/or the rearrangement of chemical bonds that must overcome a barrier, which is on the order of  $\sim \text{eV}$ , for example, by the formation of carbon chains.<sup>4,24,25</sup> Such atomic rearrangement, if elucidated in detail, may provide the basis for long-term storage. Estimates of the ultimate lifetime will require detailed understanding of the atomic motion that underlies the switching behavior. Such understating will require new experiments, such as STM studies, or observation of the switching using a transmission electron microscope.

## ■ ASSOCIATED CONTENT

### 📄 Supporting Information

In situ SEM videos showing the electrical breakdown process of few-layer suspended graphene devices. This material is available free of charge via the Internet at <http://pubs.acs.org>.

## ■ AUTHOR INFORMATION

### ✉ Corresponding Author

\*E-mail: marc.boeck@ucr.edu; lau@physics.ucr.edu.

### 👤 Author Contributions

§These authors contributed equally.

## Notes

The authors declare no competing financial interest.

## ■ ACKNOWLEDGMENTS

The authors acknowledge the support by NSF CAREER DMR/0748910, NSF DMR/1106358, NSF ECCS/0926056, ONR N00014-09-1-0724, ONR/DMEA H94003-10-2-1003 and the FENA Focus Center. CNL acknowledges the support by the “Physics of Graphene” program at KITP.

## ■ REFERENCES

- (1) Baker, M.; Shah, M.; Rosenthal, D. S. H.; Roussopoulos, M.; Maniatis, P.; Giuli, T.; Bungale, P. In Proceedings of the 1st ACM SIGOPS/EuroSys European Conference on Computer Systems 2006, Leuven, Belgium, April 18–21, 2006; Berbers, Y., Zwaenepoel, W., Eds.; ACM: New York, 2006, p 221.
- (2) Begtrup, G. E.; Gannett, W.; Yuzvinsky, T. D.; Crespi, V. H.; Zettl, A. *Nano Lett.* **2009**, *9*, 1835.
- (3) Svensson, K.; Olin, H.; Olsson, E. *Phys. Rev. Lett.* **2004**, *93*, 145901.
- (4) Standley, B.; Bao, W. Z.; Zhang, H.; Bruck, J.; Lau, C. N.; Bockrath, M. *Nano Lett.* **2008**, *8*, 3345.
- (5) Li, Y.; Sinitskii, A.; Tour, J. M. *Nat. Mater.* **2008**, *7*, 966.
- (6) Yao, J.; Zhong, L.; Zhang, Z.; He, T.; Jin, Z.; Wheeler, P. J.; Natelson, D.; Tour, J. M. *Small* **2009**, *5*, 2910.
- (7) Yao, J.; Sun, Z.; Zhong, L.; Natelson, D.; Tour, J. M. *Nano Lett.* **2010**, *10*, 4105.
- (8) Bao, W. Z.; Miao, F.; Chen, Z.; Zhang, H.; Jang, W. Y.; Dames, C.; Lau, C. N. *Nat. Nanotechnol.* **2009**, *4*, 562.
- (9) Bolotin, K. I.; Sikes, K. J.; Jiang, Z.; Klima, M.; Fudenberg, G.; Hone, J.; Kim, P.; Stormer, H. L. *Solid State Commun.* **2008**, *146*, 351.
- (10) Du, X.; Skachko, I.; Barker, A.; Andrei, E. Y. *Nat. Nanotechnol.* **2008**, *3*, 491.
- (11) Novoselov, K. S.; Geim, A. K.; Morozov, S. V.; Jiang, D.; Zhang, Y.; Dubonos, S. V.; Grigorieva, I. V.; Firsov, A. A. *Science* **2004**, *306*, 666.
- (12) Bao, W.; Liu, G.; Zhao, Z.; Zhang, H.; Yan, D.; Deshpande, A.; LeRoy, B.; Lau, C. *Nano Res.* **2010**, *3*, 98.
- (13) Collins, P. G.; Hersam, M.; Arnold, M.; Martel, R.; Avouris, P. *Phys. Rev. Lett.* **2001**, *86*, 3128.
- (14) Chiu, H. Y.; Deshpande, V. V.; Postma, H. W. C.; Lau, C. N.; Mikó, C.; Forró, L.; Bockrath, M. *Phys. Rev. Lett.* **2005**, *95*, 226101.
- (15) Childres, I.; Jauregui, L. A.; Foxe, M.; Tian, J. F.; Jalilian, R.; Jovanovic, I.; Chen, Y. P. *Appl. Phys. Lett.* **2010**, *97*.
- (16) Xu, M.; Fujita, D.; Hanagata, N. *Nanotechnology* **2010**, *21*, 265705.
- (17) Teweldebrhan, D.; Balandin, A. A. *Appl. Phys. Lett.* **2009**, *94*.
- (18) Rueckes, T.; Kim, K.; Joselevich, E.; Tseng, G. Y.; Cheung, C. L.; Lieber, C. M. *Science* **2000**, *289*, 94.
- (19) Kinaret, J. M.; Nord, T.; Viefers, S. *Appl. Phys. Lett.* **2003**, *82*, 1287.
- (20) Lee, S. W.; Lee, D. S.; Morjan, R. E.; Jhang, S. H.; Sveningsson, M.; Nerushev, O. A.; Park, Y. W.; Campbell, E. E. B. *Nano Lett.* **2004**, *4*, 2027.
- (21) Deshpande, V. V.; Chiu, H. Y.; Postma, H. W. C.; Mikó, C.; Forró, L.; Bockrath, M. *Nano Lett.* **2006**, *6*, 1092.
- (22) Bunch, J. S.; van der Zande, A. M.; Verbridge, S. S.; Frank, I. W.; Tanenbaum, D. M.; Parpia, J. M.; Craighead, H. G.; McEuen, P. L. *Science* **2007**, *315*, 490.
- (23) Jonsson, L. M.; Nord, T.; Kinaret, J. M.; Viefers, S. *J. Appl. Phys.* **2004**, *96*, 629.
- (24) Jin, C.; Lan, H.; Peng, L.; Suenaga, K.; Iijima, S. *Phys. Rev. Lett.* **2009**, *102*, 205501.
- (25) Rinzler, A. G.; Hafner, J. H.; Nikolaev, P.; Lou, L.; Kim, S. G.; Tomanek, D.; Nordlander, P.; Colbert, D. T.; Smalley, R. E. *Science* **1995**, *269*, 1550.